A Tunable Trisection Bandpass Filter with Constant Fractional Bandwidth Based on Magnetic Coupling

Mingye Fu, Qianyin Xiang, and Quanyuan Feng

School of Information Science and Technology
Southwest Jiaotong University, Chengdu, Sichuan, 610031, China
qyxiang@swjtu.edu.cn

Abstract ─ A tunable microstrip trisection bandpass filter with source-load coupling is proposed in this paper. Magnetic cross coupling structure based on varactor loaded open ring resonators is employed. No extra capacitor is used to adjust the coupling coefficients directly. Normalized coupling matrix *M* is used to calculate the frequency response, and formulas for computing the *S* parameters based on the resonator with unconventional phase performance are given. Coupling coefficients are investigated by computing the integral of the distributed voltage/current and it is proved that the coupling coefficients can meet the requirements of constant fractional bandwidth (CFBW). Due to the magnetic cross coupled trisection structure and the electrical source-load coupling, this tunable filter has three transmission zeros at finite frequency which can effectively improve the frequency selectivity. The measurement agrees well with the simulation. The center frequency can be tuned from 1097 MHz to 1936 MHz. In this tuning range, the insertion loss varies from 7.8 dB to 4 dB. A constant fractional bandwidth of about 5% is achieved.

Index Terms ─ cross-coupling, trisection filter, tunable bandpass filter.

I. INTRODUCTION

With the fast development of wireless communications, reconfigurable RF/microwave systems, which can be used in electronic countermeasures, software defined radio and so on, are highly demanded. The tunable filter, which dynamically receives the wanted signals or rejects the interferences, is regarded as a core component in reconfigurable RF/microwave systems. For tunable bandpass filters, high frequency selectivity is vital since it can effectively restrain the near-passband interference. One approach to improve frequency selectivity is utilizing high resonators with high unloaded quality factor (Q_u) such as cavity resonators [1, 2] or SIW filters [3, 4]. For varactor-tuning microstrip bandpass filters, the resonator quality factor is relatively lower. Transmission zeros can be used for improving the frequency selectivity, and crossed coupling can bring transmission zeros by making signals transmit through different paths and cancel each other at a specified frequency [5-7].

Crossed coupling has already been widely used in fixed filters [8-12]. By applying source-load coupling, *N*th order canonical filters with *N* finite transmission zeros can be achieved [10]. Recently, tunable cross-coupled tunable filters have been reported. The roll-off rate of second order tunable cross-coupled filter based on source-load cross coupling [13, 14] is limited, and several fourth order cross-coupled filters with higher frequency selectivity have been reported [6, 7, 15, 16]. In [6, 7, 15-17], tunable capacitors are placed in the coupling region for tuning the electric coupling coefficient directly, and bandwidth becomes tunable since coupling coefficients can be tuned. However, this method requires more capacitors, which may lead to higher insertion loss and increase the difficulty of practical layout design. Meanwhile, tunable capacitors which are now available on the market are relatively large as coupling capacitor. Therefore, the capacitance in resonators should be very large to maintain a relatively small coupling coefficient [6]. Tunable third order filter is a useful topology to reduce the designing difficulty and maintain the roll-off rate [18-20]. A typical third order filter is trisection filter which is desirable for some applications requiring only a higher selectivity on one side of the passband due to the advantage of its asymmetrical frequency response. [18-20] reported several third order tunable filters but they only have one or two transmission zeros. Combining cross coupled trisection structure with source-load cross coupling can bring three transmission zeros.

Open ring resonators (ORRs) are common used in microstrip filters [8, 21-23]. It can be utilized for designing tunable filters by adding a tunable capacitor at the open ends of the microstrip line. At the resonant frequency, the magnetic energy is mainly stored in the middle of the microstrip line while the majority of electrical energy is stored at the terminal region of the microstrip line and the capacitor. The larger the capacitance, the less electrical energy there is in the microstrip line, therefore, the electrical coupling can

Submitted On: August 23, 2018
Accepted On: October 23, 2019

not make the fractional bandwidth of tunable filter keep in constant.

In this paper, magnetic coupling structure based on varactor loaded ORRs are utilized to design tunable trisection filter with constant fractional bandwidth. Formulas for computing the *S* parameters based on the resonator with unconventional phase performance are given. Coupling coefficients are investigated by computing the integral of the distributed voltage/current. All-magnetic cross coupled resonators and source to load electric coupling are designed to generate three transmission zeros for improving the frequency selectivity.

II. FILTER SYNTHESIS

The most important parameters that influence filter bandwidth are coupling coefficient k and external quality factor Q_{ext}. In order to attain the desired k and Q_{ext} for constant fractional bandwidth, filter synthesis can be applied based on normalized coupling matrix M [8, 24-26]. The formulas for calculating the lowpass S parameters based on M matrix can be written as [8]:

$$\begin{cases} S_{21} = -2jA^{-1}_{n+2,1} \\ S_{11} = 1 + 2jA^{-1}_{1,1} \end{cases}, \tag{1}$$

where n is the order of the filter, $A_{i,j}^{-1}$ denotes the i^{th} row and j^{th} column element of A^{-1}, which is given by:

$$A = M + \Omega \cdot U - j \cdot q, \tag{2}$$

in which U is the (n+2) × (n+2) identity matrix except $U_{1,1} = U_{n+2,n+2} = 0$; q is a (n+2) × (n+2) matrix with all zeros except $q_{1,1} = q_{n+2,n+2} = 1$, and Ω is angular frequency. To get bandpass response, a lowpass-to-bandpass transformation can be written as:

$$\Omega = \frac{1}{FBW}\left(\frac{\omega}{\omega_0} - \frac{\omega_0}{\omega}\right), \tag{3}$$

where ω_0 is center angular frequency of the transformed bandpass filters, ω denotes angular frequency and FBW is the fractional bandwidth. The desired coupling coefficient between i^{th} and j^{th} resonators k_{ij}, and external quality factor Q_{ext}, which can determine the frequency response of the bandpass filter, can be obtained as:

$$k_{ij} = M_{ij} \bullet FBW = M_{ij}\frac{ABW}{f_0}, \tag{4}$$

$$Q_{ext} = \frac{1}{M_{S1}^{\ 2} FBW} = \frac{f_0}{M_{S1}^{\ 2} ABW}, \tag{5}$$

where M_{ij} denotes the entries in M matrix (i, j = S, 1, 2… N, L, S stands for the input source and L for the output load. The filter is Nth order), f_0 is the center frequency and ABW is the absolute bandwidth.

Figure 1 is the topology used for designing the tunable filter in this paper, where, E stands for electrical coupling and M is magnetic coupling. 1~3 denote resonator 1 to resonator 3. There are three paths from source to load, and the M matrix in (6) is used for computing the frequency response, as in Fig. 2. This topology can generate three transmission zeros at finite frequency,

$$M = \begin{pmatrix} 0 & 1.3 & 0 & 0 & -0.005 \\ 1.3 & 0 & 0.78 & 0.58 & 0 \\ 0 & 0.78 & 0 & 0.78 & 0 \\ 0 & 0.58 & 0.78 & 0 & 1.3 \\ -0.005 & 0 & 0 & 1.3 & 0 \end{pmatrix}. \tag{6}$$

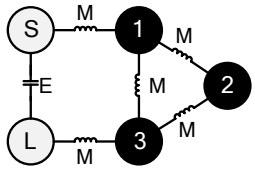

Fig. 1. The topology of the trisection bandpass filter.

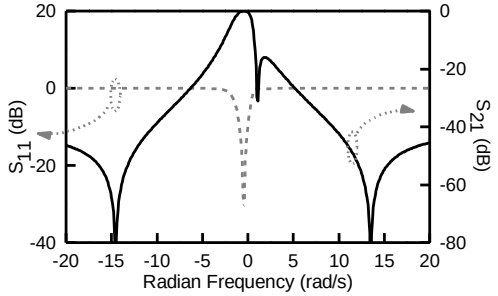

Fig. 2. The frequency response of the M matrix.

In the traditional synthesis method, the resonators have a phase shift of π/2 at low frequency and -π/2 at high frequency [26]. Figure 3 shows that the phase shift of varactor loaded ORR is opposite. Hence the U in (2) should be changed to:

$$U = diag[0, -1, -1, -1, 0]. \tag{7}$$

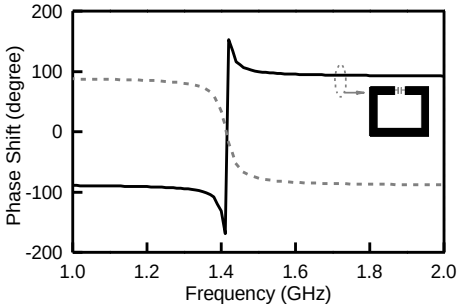

Fig. 3. The phase response of varactor loaded ORR (black solid line), and the resonators in traditional synthesis method (gray dashed line).

Figure 4 shows the response based on the topology shown in Fig. 1 based on the varactor loaded ORR, with

FBW = 0.05 under center frequency of 1.3 GHz, 1.5 GHz, and 1.7 GHz, respectively. The desired coupling coefficients and external quality factor versus center frequency can be calculated using (4) and (5), as shown in Fig. 2.

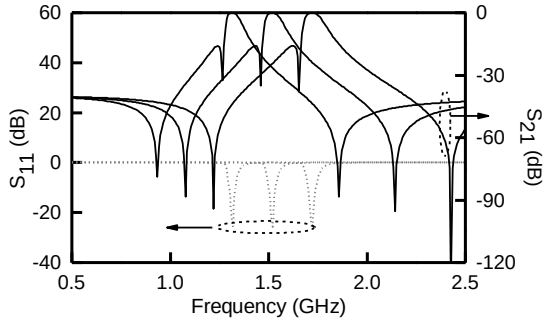

Fig. 1. Bandpass response of the *M* matrix. This calculation uses the modified *U*.

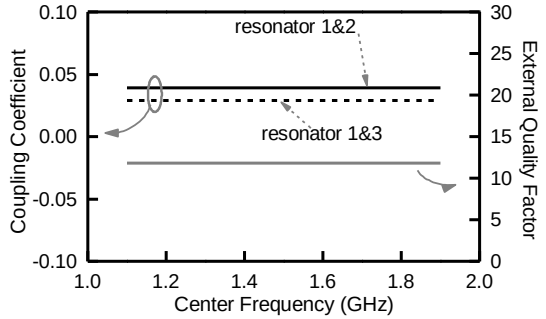

Fig. 2. The desired coupling coefficients and external quality factor extracted from *M* matrix.

III. FILTER DESIGN

Figure 6 shows the tunable cross coupled trisection bandpass filter based on the magnetic coupled varactor loaded ORR. D_1~D_6 are the varactors and R_1~R_6 are 5.1 kΩ resistors used as RF chokes. Feedlines utilize magnetic coupling to achieve matching and electrical source-load coupling is implemented through feedlines. Table 1 lists their physical parameters in Fig. 6. Three types of geometry parameters are used for studying the coupling structure.

A. Coupling coefficients

The relationship between center angular frequency ω_0 and the equivalent capacitance of varactors can be analyzed by half circuit of the resonators. For resonator 1 and resonator 3 in Fig. 6, their half circuit is shown in Fig. 7 (a). It is made up with two short ended microstrip lines and two capacitors named C_L. Y_0 is the characteristic admittance of the microstrip lines, θ_1 is the electrical length of the coupling region and θ_2 is the electrical length of each microstrip line.

At resonating frequency ω_0, the tunable capacitance C_L can be written as:

$$j\omega C_L - jY_0 \cot\theta_2 = 0\,, \tag{8}$$

$$C_L = \frac{Y_0 \cot\theta_2\big|_{\omega=\omega_0}}{\omega_0}\,. \tag{9}$$

The calculated curves of the tunable capacitor C_L versus center frequency based on the three geometries in Table 1 are shown in Fig. 8. Since L_2, L_3 and W_2 of the three geometries are same, the calculated curves coincide.

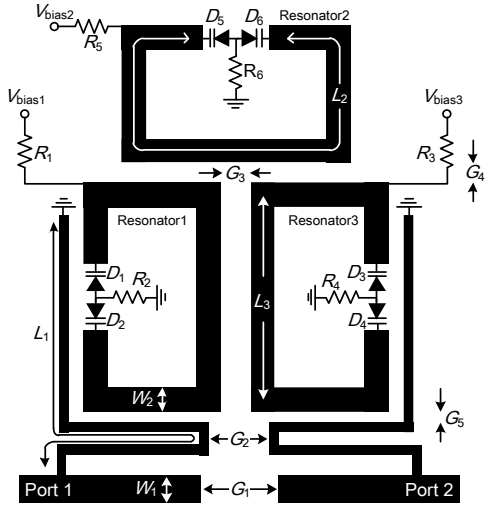

Fig. 6. The electrical circuit model of this filter.

Table 1: Physical parameters of 3rd tunable filters

Parameters (unit: mm)	Dimension 1	Dimension 2	Dimension 3
L_2	26.9	26.9	26.9
L_3	11.1	11.1	11.1
W_2	0.7	0.7	0.7
G_3	1.8	2	2.2
G_4	0.4	0.6	0.8

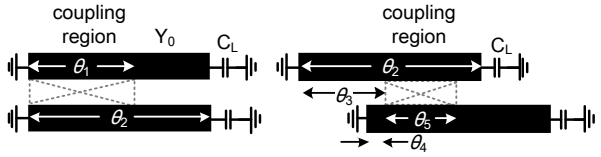

Fig. 7. The equivalent model of half circuit of coupled resonators: (a) resonator 1 and 3, and (b) resonator 1 and 2.

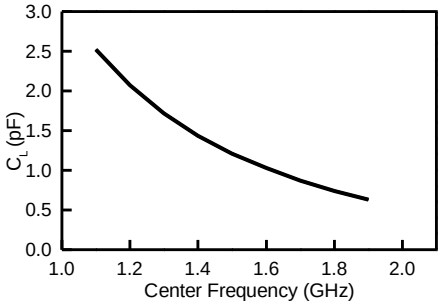

Fig. 8. The calculated C_L versus center frequency.

Coupling coefficients can be analyzed by energy method used in [18, 27]. In the half circuit of resonator 1 and 3 shown in Fig. 7 (a), the electrical energy and magnetic energy stored in each resonator at center frequency can be written as:

$$W_{C_1} = W_{L_1} = W_{C_3} = W_{L_3} = \frac{1}{2} L Y_0^2 \int_0^{\theta_2} \cos^2 \theta d\theta , \quad (10)$$

where W_{Li} (i = 1, 3) denotes magnetic energy in i^{th} resonator, W_{Ci} (i = 1, 3) denotes electric energy in i^{th} resonator, L is the self-inductance of the microstrip lines. Meanwhile, the magnetic energy stored in the coupling region, W_{Lm}, is expressed as:

$$W_{L_m} = L_m Y_0^2 \int_0^{\theta_1} \cos^2 \theta d\theta . \quad (11)$$

L_m is the mutual inductance between the two lines. Therefore, the magnetic coupling coefficient of this half circuit is obtained by the energy relationship:

$$k_L = \frac{W_{L_m}}{2\sqrt{W_{L_1} W_{L_3}}} . \quad (12)$$

The electrical energy stored in coupling region is,

$$W_{C_m} = -C_m \int_0^{\theta_1} \sin^2 \theta d\theta . \quad (13)$$

C_m is the mutual capacitance between the two lines. So electrical coupling coefficient can be calculated:

$$k_C = \frac{W_{C_m}}{2\sqrt{W_{C_1} W_{C_3}}} . \quad (14)$$

The total coupling coefficient of this half circuit is the sum of k_C and k_L, which is,

$$k = k_L + k_C . \quad (15)$$

As for resonator 1 and resonator 2, the half circuit is shown in Fig. 7 (b). Energy stored in each resonator can be calculated using (10). However, the formula to get energy stored in coupling region should be modified:

$$W_{L_m} = L_m Y_0^2 \int_{\theta_3}^{\theta_2} \cos\theta \cos\left(\theta - (\theta_3 - \theta_4)\right) d\theta , \quad (16)$$

$$W_{C_m} = -C_m \int_{\theta_3}^{\theta_2} \sin\theta \sin\left(\theta - (\theta_3 - \theta_4)\right) d\theta . \quad (17)$$

Rewrite (12) and (14) as:

$$k_L = \frac{W_{L_m}}{2\sqrt{W_{L_1} W_{L_2}}} , \quad (18)$$

$$k_C = \frac{W_{C_m}}{2\sqrt{W_{C_1} W_{C_2}}} . \quad (19)$$

For the entire resonators, the energy stored in each resonator is doubled, yet the energy stored in the coupling region does not change. As a result, the coupling coefficient between resonator 1 and 2 is equal to k/2. The coupling coefficients versus center frequency can be calculated by using (9) ~ (19), as shown in Fig. 9 (a) and Fig. 9 (b). It shows that, the strength of coupling can be controlled by adjusting its physical parameters, and the geometry parameters of Dimension 2 in Table 1 will be implemented in the design so that a 5% constant FBW (CFBW) can be achieved.

Simulation is carried out to verify the above calculation. f_1 and f_2 are the splitting resonate frequencies in the simulation, and the coupling coefficient k can be calculated as:

$$k = \frac{f_1^2 - f_2^2}{f_1^2 + f_2^2} . \quad (20)$$

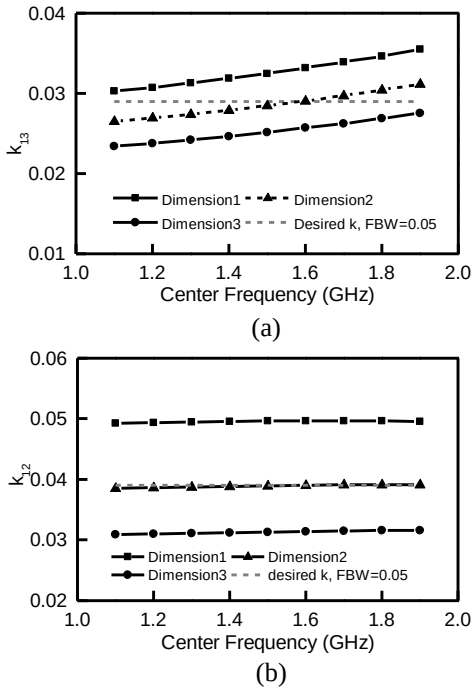

Fig. 9. The calculated results versus center frequency: (a) coupling coefficient k_{12}, and (b) coupling coefficient k_{13}.

Figure 10 shows the simulated loaded capacitance versus center frequency compared with calculated results. It shows that the center frequency can be tuned from 1.1 GHz to almost 2 GHz when C_L is tuned from 0.6 pF to 2.4 pF, and the calculation matches the simulation very well. The slope of coupling coefficient curves is very small, which meets the requirement of

CFBW response.

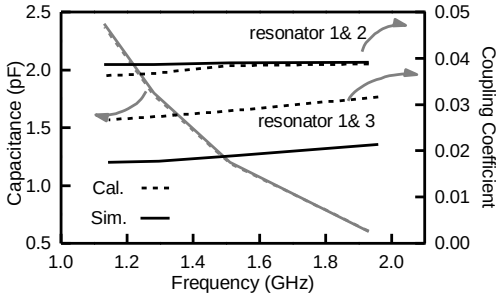

Fig. 10. The tunable capacitance and coupling coefficients versus center frequency of calculation and simulation.

B. External quality factor

External quality factor Q_{ext} mainly influences the bandwidth, roll-off, inband ripple. For tunable filters with CFBW, Q_{ext} needs to be constant. It can be gotten by simulating single loaded circuits shown in Fig. 11 (a) [8], and Q_{ext} can be calculated as:

$$Q_{ext} = \frac{2\pi f_0 \tau_{S11}}{4}, \tag{21}$$

or,

$$Q_{ext} = \frac{f_0}{\Delta f_{\pm\pi/20}} = \frac{f_0}{f_{-\pi/2} - f_{+\pi/2}}, \tag{22}$$

where τ_{s11} is group delay of S_{11}, $f_{\pi/2}$ and $f_{-\pi/2}$ are frequency point at which the phase of S_{11} of the one-terminal network in Fig. 11 (a) is $\pm\pi/2$, respectively.

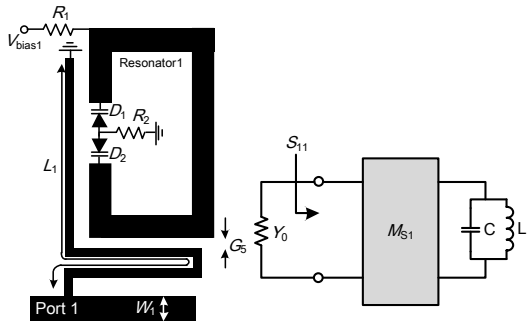

(a) (b)

Fig. 11. The simulation circuit and its equivalent model.

L_1=25 mm, W_1=2.2 mm and other parameters except G_5 are kept as in dimension 2 mentioned earlier. The gap between feedline and resonator can influence Q_{ext}. We simulated four conditions that G_5 in Fig. 11 (a) is 0.05 mm, 0.1 mm, 0.2 mm and 0.3 mm, respectively. The simulated external quality factors are shown in Fig. 12. When G_5 increases, Q_{ext} decreases. This can be explained by the equivalent model in Fig. 11 (b). At $f_{-\pi/2}$ or $f_{\pi/2}$, we have:

$$Y_0 = \left| j\frac{2\pi f_{\pm\pi/2} L M_{S1}^{\ 2}}{1-(2\pi f_{\pm\pi/2})^2 LC} \right|, \tag{23}$$

because,

$$S_{11} = \frac{Y_0 - j\dfrac{\omega L M_{S1}^{\ 2}}{1-\omega^2 LC}}{Y_0 + j\dfrac{\omega L M_{S1}^{\ 2}}{1-\omega^2 LC}} \tag{24}$$

By solving equation (23), the denominator of equation (22) is attained:

$$f_{-\pi/2} - f_{+\pi/2} = \frac{M_{S1}^2}{2\pi C Y_0}. \tag{25}$$

Substituting (25) into (22), the external quality of the circuits in Fig. 11 (b) is:

$$Q_{ext} = \frac{CY_0}{M_{S1}^2\sqrt{LC}}. \tag{26}$$

when the gap becomes narrower, the coupling is enhanced so $|M_{S1}|$ increases. Equation (26) implies that the external quality factor will decrease if C and L are constant (i.e., f_0 is fixed). When G_5 equals to 0.1 mm, the external quality factor is the closest to the desired value. Q_{ext} is also required to be unchangeable for CFBW filters and the simulated results satisfy this requirement.

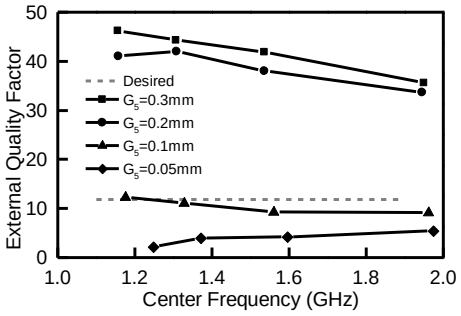

Fig. 12. Simulated external quality factor versus center frequency.

C. Source-load coupling

S_{21} of lowpass prototype filter at $\Omega = \infty$ can be written as [26]:

$$S_{21\infty} = \frac{2|M_{SL}|}{1+M_{SL}^2}. \tag{27}$$

If the coupling of source-load is enhanced, $|M_{SL}|$ will increase, and $S_{21\infty}$ increases when $|M_{SL}| < 1$. The electric type M_{SL} of this filter is desired to be -0.005 for a 40-dB rejection level. M_{SL} can be simulated by removing all resonators. A two-port network consisting of only two feed lines is obtained as shown in Fig. 13. The image part of Y_{12} of the network is used to extract M_{SL} [28] since Y_{12} denotes a J inverter with J=Im(Y_{12}):

$$M_{SL} = \mathrm{Im}(Y_{12}) \times 50. \tag{28}$$

The simulation is carried out when G_1 (other parameters in Fig. 6 are fixed, G_2=2.4 mm) is varying. Figure 14 shows the different Im(Y_{12}). It is obvious that |Im(Y_{12})| is negatively relative to G_1. |Im(Y_{12})| is controllable so it is possible to meet desired |M_{SL}| by adjusting the gap. Finally, G_1 is chosen to be 3.4 mm.

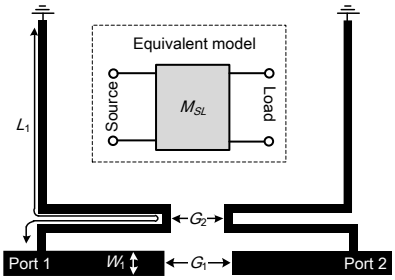

Fig. 13. The simulation circuit of M_{SL}.

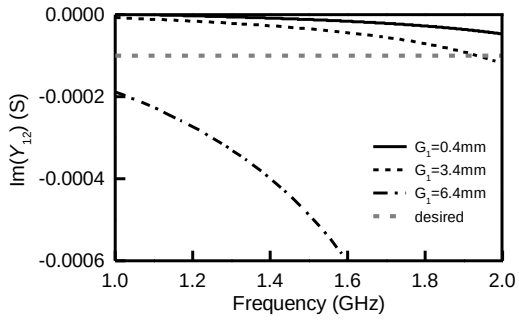

Fig. 14. The simulated imaginary of Y_{12}.

IV. FILTER SIMULATION

A layout of the filter is designed and simulated. The substrate with h = 0.8 mm, ε_r = 2.65, tanδ = 0.001, and SMV1405 varactor diode are utilized. Figure 15 shows the S parameters under 0V, 1V, 3V, 7V, 14V and 30V bias voltages.

The center frequency varies from 1086MHz to 1941 MHz which means a 179% tuning range is achieved. As shown in Fig. 16, in the tuning range, fractional bandwidth of this filter keeps almost unchangeable (4.25% ~4.73%) and the insertion loss is less than 6.2 dB. Additionally, there are three transmission zeros besides the passband. One is generated by the utilized trisection structure and is located at lower edge of the passband. The other two transmission zeros exist at each edge of the passband due to the source-load coupling. These zeros can improve the selectivity of this filter. The rejection is approximately 40 dB (higher frequency, estimated by the frequency response's asymptote in Fig. 15) or higher than 50 dB (lower frequency, estimated by the frequency response's stationary point in Fig. 15).

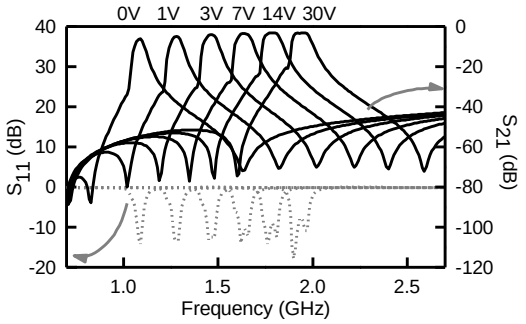

Fig. 15. Simulated S parameters under typical tuning states.

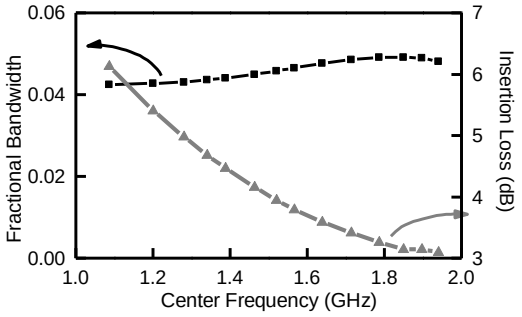

Fig. 16. Simulated insertion loss and fractional bandwidth (*FBW*).

V. FABRICATION AND MEASUREMENT

The filter is fabricated with an overall size of 36 mm × 40 mm, as shown in Fig. 17. Three lines on the sectorial pads are connected to the DC supply to bias the varactors. The frequency response of the filter is measured by Agilent E5071C vector network analyzer.

The bias voltage is swept from 0 V to 30 V and V_{bias1} = V_{bias2} = V_{bias3}. Figure 18 shows the measured S parameters with 0V, 1V, 3V, 7V, 14V, and 30V bias voltages. The measured frequency responses agree well with the simulation. The tuning ratio of center frequency is approximately 176% (1097 MHz ~ 1936 MHz). Three transmission zeros are generated, and the selectivity of this filter is improved by the transmission zeros. The rejection level is about 40 dB (higher frequency) or higher than 50 dB (lower frequency).

Figure 19 shows the measured insertion loss and fractional bandwidth. The fractional bandwidth maintains 4.1% ~5.3%. It is very narrow, which is useful for channelization. The insertion loss changes from 7.8 dB to 4 dB, which is approximately 1 dB higher than simulation. Besides the inaccuracy in PCB fabrication and the practical discrepancy between varactors, this is mainly due to the errors in welding. The PCB is relatively small in size and the gap between feedlines and resonators is very narrow. So, the solder joint,

which is not small enough to be ignored or to be regarded as ideal connection point, has a great effect on the performance. A similar situation can be seen in [29]. This is not simulated in software and can be solved by precise fabrication or lower frequency application with larger board area. Nonlinear characteristics is usually represented by IIP3 (input 3rd order intercept point), for example [29]. It can be obtained by feeding dual tone signals and measuring the output frequency spectrum. The frequencies of the input signals are set to be $f_0 \pm 1$ MHz. The tested IIP 3 is shown in Fig. 20. Table 2 shows the comparison with several recent cross-coupled tunable filters.

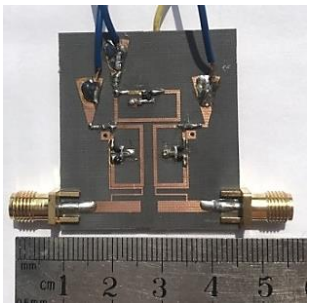

Fig. 17. The photograph of the fabricated filter.

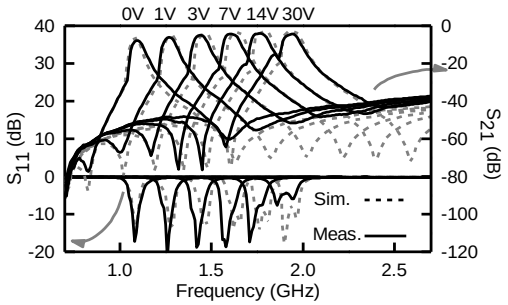

Fig. 18. The measured S parameters.

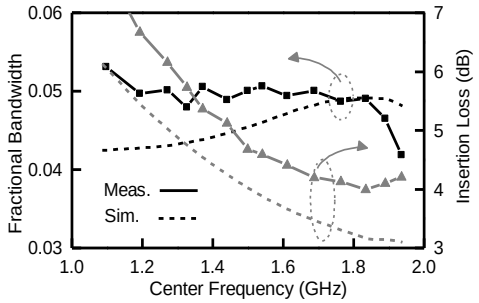

Fig. 19. The measured insertion loss and FBW of this filter.

Table 2: Comparison with recent cross-coupled tunable filters

Reference	Tuning Range (GHz)	Insertion Loss (dB)	Bandwidth	Number of Zeros
[13]	1.11~1.51	3.6~4.2	29±3MHz*, 1.8%~2.6%*	2
[14]	1.15~2	3.6~2.4	114±4MHz*, 9.9%~5.7%*	2
[15]	1.5~1.75	4.5~11	variable	2
[16]	1.25~2.1	3.5~8.5@FBW=4% 3.5~6.5@FBW=5.5%	variable	2
[19]	0.41~0.82	<6.5	9±1%	1
[30]	0.95~1.46	1.8~3.6	12.5±2%	3
[31]	1.36~1.78	2.8~5	93±7 MHz	2
This work	1.097~1.936	7.8~4	4.7±0.6%	3

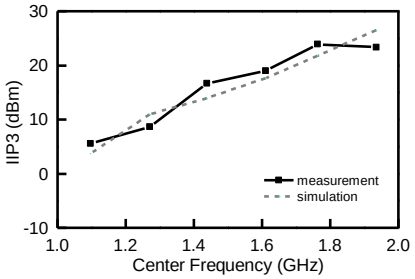

Fig. 20. The measured IIP3 compared with simulation.

It should be noted that the default bandwidth is 3dB bandwidth while the marked data using the symbol * is 1 dB bandwidth in Table 2. Different from the 3rd order filter in [30] with 3 transmission zeros, this crossed coupled filter does not require additional coupling coefficient tuning elements. This is also an advantage when competing with 4th order filter in [15, 16]. Filter in [31] do not need additional capacitors, either, but it needs two different bias voltage values while in this filter only need one bias voltage value.

VI. CONCLUSION

In this paper, a cross coupled tunable trisection filter with source-load coupling is proposed. All magnetic coupling is employed in trisection structure while source and load are electrically coupled. Three transmission zeros that can effectively improve the frequency selectivity are generated due to the crossed coupled topology. *M* matrix is used to guide this design. The phase performance of the resonator is studied then

the computing formula of *S* parameters based on *M* is modified for this resonator. Energy relationship is utilized to analyze the coupling coefficients, which proves that the designed structures are able to satisfy the requirements of CFBW. According the theoretical analysis, coupling coefficients can be controlled and meet the desired values. Source-load coupling, and external quality factor are studied, optimized by simulation. The filter is fabricated on F4B-2 substrate and measured by a vector network analyzer. The measurement matches the simulation well. The tuning range is 1097 MHz to 1936 MHz, meaning that a 176% tuning ratio is achieved. The fractional bandwidth is keeping about 5%. In tuning range, the insertion loss varies from 7.8 dB to 4 dB.

ACKNOWLEDGMENT

This work is supported by the National Natural Science Foundation of China (NSFC) under Grant 61771408, 61401375, 61531016, the Fundamental Research Funds for the Central Universities under Grant 2682014RC24, and the Sichuan Provincial Science and Technology Important Projects under Grant 2018GZ0139, 2017GZ0110.

REFERENCES

[1] S. Nam, B. Lee, C. Kwak, and J. Lee, "A new class of k-band high-q frequency-tunable circular cavity filter," *IEEE Transactions on Microwave Theory and Techniques*, vol. 66, no. 3, pp. 1228-1237, 2018.

[2] B. Yassini, M. Yu, and B. Keats, "A ka-band fully tunable cavity filter," *IEEE Transactions on Microwave Theory and Techniques*, vol. 60, no. 12, pp. 4002-4012, 2012.

[3] H. Aghayari, N. Komjani, and N. M. Garmjani, "A novel integrated corrugated waveguide bandpass filter," *Applied Computational Electromagnetics Society Journal*, vol. 27, no. 1, pp. 67-73, Jan. 2012.

[4] G. Zhang, J. P. Wang, H. Gu, and X. Xu, "60-ghz 3-d cavity bandpass filter for v-band gigabit wireless systems," *Applied Computational Electromagnetics Society Journal*, vol. 29, no. 11, pp. 928-933, Nov. 2014.

[5] S. Zhang, L. Zhu, and R. Weerasekera, "Synthesis of inline mixed coupled quasi-elliptic bandpass filters based on lamda/4 resonators," *IEEE Transactions on Microwave Theory and Techniques*, vol. 63, no. 10, pp. 3487-3493, 2015.

[6] A. Anand and X. Liu, "Reconfigurable planar capacitive coupling in substrate-integrated coaxial-cavity filters," *IEEE Transactions on Microwave Theory and Techniques*, vol. 64, no. 8, pp. 2548-2560, 2016.

[7] Y. C. Chiou and G. M. Rebeiz, "Tunable 1.55 - 2.1 ghz 4-pole elliptic bandpass filter with bandwidth control and > 50 db rejection for wireless systems," *IEEE Transactions on Microwave Theory and Techniques*, vol. 61, no. 1, pp. 117-124, 2013.

[8] J. Hong, *Microstrip Filters for RF Microwave Applications*, 2nd Edition, NY:Wiley, New York, 2001.

[9] T. Saito, S. Kodama, S. Ohshima, and A. Saito, "Design of high power handling filter using cascaded quadruplet superconducting bulk resonators," *IEEE Transactions on Applied Superconductivity*, vol. 28, no. 4, pp. 1-4, 2018.

[10] X. Jun, H. Wei, and C. Zhe, "A compact quarter-wavelength stepped-impedance resonator bandpass filter with source-load coupling," *2015 IEEE International Wireless Symposium (IWS 2015)*, pp. 1-4, Mar. 30-Apr. 1, 2015.

[11] B. Liu, Z. Guo, X. Wei, Y. Ma, R. Zhao, K. Xing, and L. Wu, "Quad-band bpf based on slrs with inductive source, and load coupling," *Electronics Letters*, vol. 53, no. 8, pp. 540-542, 2017.

[12] N. M. Garmjani and N. Komjani, "Improved microstrip folded tri-section stepped impedance resonator bandpass filter using defected ground structure," *Applied Computational Electromagnetics Society Journal*, vol. 25, no. 11, pp. 975-983, Nov. 2010.

[13] D. Tian, Q. Feng, and Q. Xiang, "A constant absolute bandwidth tunable band-pass filter based on magnetic dominated mixed coupling, and source-load electric coupling," *Journal of Electromagnetic Waves, and Applications*, vol. 30, no. 15, pp. 1953-1963, 2016.

[14] D. Lu, N. S. Barker, and X. Tang, "A simple frequency-agile bandpass filter with predefined bandwidth and stopband using synchronously tuned dual-mode resonator," *IEEE Microwave and Wireless Components Letters*, vol. 27, no. 11, pp. 983-985, 2017.

[15] C. Schuster, R. Hu, A. Wiens, M. Maasch, R. Jakoby, and H. Maune, "Cross-coupled open-loop resonator bandpass filter with independently tunable center frequency and bandwidth," *2018 IEEE Radio and Wireless Symposium (RWS)*, pp. 52-55, 15-18 Jan. 2018.

[16] T. Yang and G. M. Rebeiz, "Tunable 1.25-2.1-ghz 4-pole bandpass filter with intrinsic transmission zero tuning," *IEEE Transactions on Microwave Theory and Techniques*, vol. 63, no. 5, pp. 1569-1578, 2015.

[17] L. Zhou, S. Liu, J. Duan, and M. Xun, "A novel tunable combline bandpass filter based on external quality factor and internal coupling tunings," *Applied Computational Electromagnetics Society Journal*, vol. 33, no. 6, pp. 690-696, Jun.

2018.
[18] Z. Zhao, J. Chen, L. Yang, and K. Chen, "Three-pole tunable filters with constant bandwidth using mixed combline, and split-ring resonators," *IEEE Microwave and Wireless Components Letters*, vol. 24, no. 10, pp. 671-673, 2014.
[19] M. Y. Fu, Q. Y. Xiang, D. Zhang, D. Y. Tian, and Q. Y. Feng, "A uhf 3rd order 5-bit digital tunable bandpass filter based on mixed coupled open ring resonators," *2016 Progress in Electromagnetic Research Symposium (PIERS)*, pp. 3460-3463, 8-11 Aug. 2016.
[20] Y. C. Chiou and G. M. Rebeiz, "A tunable three-pole 1.5-2.2-ghz bandpass filter with bandwidth, and transmission zero control," *IEEE Transactions on Microwave Theory and Techniques*, vol. 59, no. 11, pp. 2872-2878, 2011.
[21] Y. Chu-Chen, and C. Chi-Yang, "Microstrip cascade trisection filter," *IEEE Microwave and Guided Wave Letters*, vol. 9, no. 7, pp. 271-273, 1999.
[22] R. Kaushik, M. G. Madhan, and K. Jagadeeshvelan, "Design and development of microstrip trisection filter for dth applications," *2014 International Conference on Communication and Network Technologies*, pp. 8-10, 18-19 Dec. 2014.
[23] Q. Xiang, Q. Feng, and X. Huang, "Tunable bandstop filter based on split ring resonators loaded coplanar waveguide," *Applied Computational Electromagnetics Society Journal*, vol. 28, no. 7, pp. 591-596, Jul. 2013.
[24] R. J. Cameron, "Advanced coupling matrix synthesis techniques for microwave filters," *IEEE Transactions on Microwave Theory and Techniques*, vol. 51, no. 1, pp. 1-10, 2003.
[25] R. J. Cameron, "General coupling matrix synthesis methods for chebyshev filtering functions," *IEEE Transactions on Microwave Theory and Techniques*, vol. 47, no. 4, pp. 433-442, 1999.
[26] R. J. Cameron, "Advanced filter synthesis," *IEEE Microwave Magazine*, vol. 12, no. 6, pp. 42-61, 2011.
[27] A. C. Guyette, "Alternative architectures for narrowband varactor-tuned bandpass filters," *2009 European Microwave Integrated Circuits Conference (EuMIC)*, pp. 475-478, 28-29 Sept. 2009.
[28] M. Ohira and Z. Ma, "A parameter-extraction method for microwave transversal resonator array bandpass filters with direct source/load coupling," *IEEE Transactions on Microwave Theory and Techniques*, vol. 61, no. 5, pp. 1801-1811, 2013.
[29] T. Lin, K. K. W. Low, R. Gaddi, and G. M. Rebeiz, "High-linearity 5.3-7.0 ghz 3-pole tunable bandpass filter using commercial rf mems capacitors," *2018 48th European Microwave Conference (EuMC)*, pp. 555-558, 23-27 Sept. 2018.
[30] D. Jia, Q. Feng, X. Huang, and Q. Xiang, "Tunable microstrip bandpass filter with constant fractional bandwidth based on cascade triplet topology," *International Journal of Electronics*, vol. 104, no. 10, pp. 1646-1657, 2017.
[31] S. Wang, Q. Xiang, and Q. Feng, "A fourth order constant absolute bandwidth tunable bandpass filter with cross-coupling," *2019 IEEE MTT-S International Wireless Symposium (IWS)*, pp. 1-3, 19-22 May 2019.

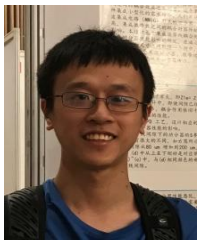

Mingye Fu received the B.S. degree from Southwest Jiaotong University, Chengdu, China in 2017. He is now studying for Ph.D. degree in Southwest Jiaotong University, focusing on the microwave technology. His research interests include the reconfigurable/tunable RF circuits, MMIC/RFIC design.

Qianyin Xiang received the B.Eng. degree in Communication Engineering, and Ph.D. degree in Communication, and Information Systems from Southwest Jiaotong University (SWJTU), Chengdu, China, in 2005 and 2013, respectively. Xiang is member of *Applied Computational Electromagnetics Society*, *Institute of Electrical and Electronics Engineers (IEEE)*, and *IEEE Microwave Theory and Techniques Society (MTT-S)*. His research interests include Analog/RF circuits and systems, tunable/software defined devices, MMIC/RFIC.

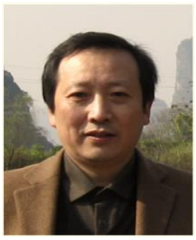

Quanyuan Feng received the M.S. degree in Microelectronics, and Solid Electronics from University of Electronic Science and Technology of China (UESTC), and the Ph.D. degree in Electromagnetic Feld and Microwave Technology from Southwest Jiaotong University (SWJTU), Chengdu, China, in 1991 and 2000, respectively. Prof. Feng has been honored as the "Excellent Expert" and the "Leader of Science and Technology" of Sichuan for his outstanding contribution. His research interests include antennas and propagation, integrated circuits design, electromagnetic compatibility and environmental electromagnetics, microwave materials and devices.